Detecting Solvent-Driven Transitions of poly(A) to Double-Stranded Conformations by Atomic Force Microscopy

Changhong Ke,[†‡] Anna Loksztejn,[†§] Yong Jiang,[†] Minkyu Kim,[†] Michael Humeniuk,[†] Mahir Rabbi,[†] and Piotr E. Marszalek[†*]

[†]Department of Mechanical Engineering and Materials Science, Center for Biologically Inspired Materials and Material Systems, Duke University, Durham, North Carolina; [‡]Department of Mechanical Engineering, State University of New York at Binghamton, New York; and [§]Department of Chemistry, University of Warsaw, Warsaw, Poland

ABSTRACT We report the results of direct measurements by atomic force microscopy of solvent-driven structural transitions within polyadenylic acid (poly(A)). Both atomic force microscopy imaging and pulling measurements reveal complex strand arrangements within poly(A) induced by acidic pH conditions, with a clear fraction of double-stranded molecules that increases as pH decreases. Among these complex structures, force spectroscopy identified molecules that, upon stretching, displayed two distinct plateau features in the force-extension curves. These plateaus exhibit transition forces similar to those previously observed in native double-stranded DNA (dsDNA). However, the width of the first plateau in the force-extension curves of poly(A) varies significantly, and on average is shorter than the canonical 70% of initial length corresponding to the B-S transition of dsDNA. Also, similar to findings in dsDNA, stretching and relaxing elasticity profiles of dspoly(A) at forces below the mechanical melting transition overlap but reveal hysteresis when the molecules are stretched above the mechanical melting transition. These results strongly suggest that under acidic pH conditions, poly(A) can form duplexes that are mechanically stable. We hypothesize that under acidic conditions, similar structures may be formed by the cellular poly(A) tails on mRNA.

INTRODUCTION

In eukaryotic cells mRNA is modified at its 3′ end by a stretch of ~200 adenines. This long adenine tail affects mRNA stability and participates in critical processes such as mRNA transportation to the cytoplasm and initiation of translation (1). Because of the biological significance of polyadenylate sequences, polyadenylic acid (poly(A)) has received a great deal of attention in numerous structural studies (reviewed by Petrovic et al. (2)). The studies showed that poly(A) may exist in two secondary structures (2). In the alkaline and neutral pH environment, poly(A) forms right-handed, single-stranded helical structures stabilized by strong base-stacking interactions among adenines (3–6). Under acidic pH conditions, poly(A) is believed to form right-handed, double-stranded helical structures with two parallel chains and stacked bases. This double helix is stabilized by electrostatic interactions between the proton at the N_1 atom of adenines and negatively charged phosphate groups (7,8). The transition of poly(A) from a single helix to a double helix can be induced by changes of pH (9). It was recently proposed that double-stranded poly(A) (dspoly(A)) structures can be formed in a living cell upon mRNA polyadenylation through intra- or interstrand associations. It was further postulated that the mechanical properties of such a double-stranded helix may be involved in the termination of poly(A) synthesis and may also affect a number of other activities (10). However, to the best of our knowledge, such dspoly(A) structures have never been examined at a single-molecule level.

In this study we report the results of atomic force microscopy (AFM) imaging and force spectroscopy measurements that captured acidic pH-induced poly(A) structures and determined their mechanical fingerprints. We compare the nanomechanics of dspoly(A) with that of double-stranded DNA (dsDNA), which has been thoroughly characterized by numerous studies using a variety of single-molecule manipulation techniques (11–23).

MATERIALS AND METHODS

Materials

Single-stranded poly(A) (product P9403) and single-stranded poly(dT) (product P6905) were purchased from Sigma-Aldrich (St. Louis, MO). Both poly(A) and poly(dT) were originally in the form of powders. Based on the data from the manufacturer, the molecule length of poly(A) and poly(dT) are polydispersed, with the majority of molecules having lengths within a range of 300–3000 bases and 600–4000 bases, respectively.

AFM imaging

1-(3-Aminopropyl)silatrane-functionalized (APS)-mica was used for binding of poly(A) molecules. The APS-mica was prepared as described by Shlyakhtenko et al. (24). A drop of 30–50 μL of poly(A) solution at a concentration of 5–40 ng/μL in TE buffer (pH 8.0), citrate buffer (pH 5.5), or citrate buffer (pH 4.8) supplemented with 150 mM NaCl was deposited on the APS-mica surface at room temperature for 5 min. The sample was rinsed with buffer and air-dried before imaging. Images were taken with a Nanoscope IIIa Multi-Mode scanning probe microscope (Veeco Instruments, Santa Barbara, CA) using tapping mode with an E scanner. RTESP probes (Veeco) were used for imaging in air. The spring constant of the AFM cantilevers was 20–80 N/m, and their resonance frequency was 275–316 kHz. The images were collected at a scan rate of 2.0–3.0 Hz, a scan line of 512 × 512 pixels, and scan size of 1 μm. The heights of the poly(A) molecules were measured from flattened AFM images using Nanoscope software (ver. 5.30r3; Veeco).

Submitted July 10, 2008, and accepted for publication December 19, 2008.

*Correspondence: pemar@duke.edu

All authors contributed equally to this work.

Editor: Taekjip Ha.

0006-3495/09/04/2918/8 $2.00

doi: 10.1016/j.bpj.2008.12.3939

AFM pulling measurements

Readers interested in the technical details of single-molecule force spectroscopy as implemented on the AFM platform may find useful information in a recent publication (25). Below, we briefly describe our setup and experimental procedures. Measurements of the elasticity of poly(A) and poly(dT) were carried out in solution at room temperature on our in-house-made AFM instrument, which was designed and equipped specifically for force spectroscopy measurements (4,26,27). For force spectroscopy measurements we used nonspecific adsorption of poly(A) or poly(dT) molecules to fresh gold substrates and untreated silicon nitride AFM tips (Microlever from Veeco) (28). These cantilevers have a nominal spring constant of 10 mN/m and an actual spring constant of 15–20 mN/m, as determined using the energy equipartition approach (29). The AFM head produced a root mean-square force noise of ~8.2 pN in the 1–500 Hz bandwidth. The pulling speed for all measurements was set to 0.5 μm/s. Then 80 μL of poly(A) or poly(dT) solution (~50–80 ng/μL) in Tris-EDTA (TE) buffer (10 mM Tris+HCl, 1 mM EDTA, pH 8.0; Sigma-Aldrich) supplemented with 150 mM NaCl were deposited onto a freshly evaporated gold surface. After the sample was incubated for 2–3 h at room temperature, it was gently rinsed three to five times with the buffer solution. Alternatively, the incubated poly(A) sample was rinsed seven or eight times with Mili-Q water (pH 5.5) for measurements carried out in water. The samples of poly(A) in citrate buffer (pH 5.5, pH 4.8 or pH 4.0) supplemented with 150 mM NaCl were prepared in a similar fashion as the poly(A) in TE buffer. All of the pH values were measured using a digital pH meter (Oakton Acorn Series pH 6 meter; Sigma-Aldrich). The plateau forces were measured in the middle of the plateau width, and the values presented are in the format of mean value $\pm$ standard error of the mean.

RESULTS

We examined the structural configuration of poly(A) in acidic and mildly alkaline pH conditions by imaging the topography of poly(A) molecules using AFM. We also investigated the elasticity of poly(A) under both mildly alkaline and acidic conditions by stretching these polymers using AFM.

AFM imaging of poly(A) under mildly alkaline pH conditions

We performed AFM imaging of poly(A) deposited on the APS-mica surface from TE buffer supplemented with 150 mM NaCl, at a pH of 8.0. We quantified the height distribution of poly(A) under these conditions. One representative image is shown in Fig. 1 *A*. Fig. 1 *B* shows the height histogram of 100 poly(A) molecules captured in four different images. The distribution is quite narrow, indicating the presence of one conformational population. The average height of poly(A) molecules in alkaline TE buffer is 0.59 $\pm$ .013 nm. This result is consistent with poly(A) being in a single-stranded conformation.

The elasticity of poly(A) in a single-helix configuration

A representative force-extension profile of poly(A) obtained in Tris-EDTA (TE) buffer, pH 8.0, 150 mM NaCl, is shown in red (*gray* in print) in Fig. 1 *C*. The curve displays a quasi-plateau feature at 24 $\pm$ 1 pN ($n = 11$; *red arrow*) extending the length of the polymer by ~80%. This plateau likely represents severing of base-stacking interactions among adenines in a single-stranded helix, and these results are consistent with the results recently reported for poly(A) by Seol et al. (5) and for poly(dA) by Ke et al. (4). The plateau feature

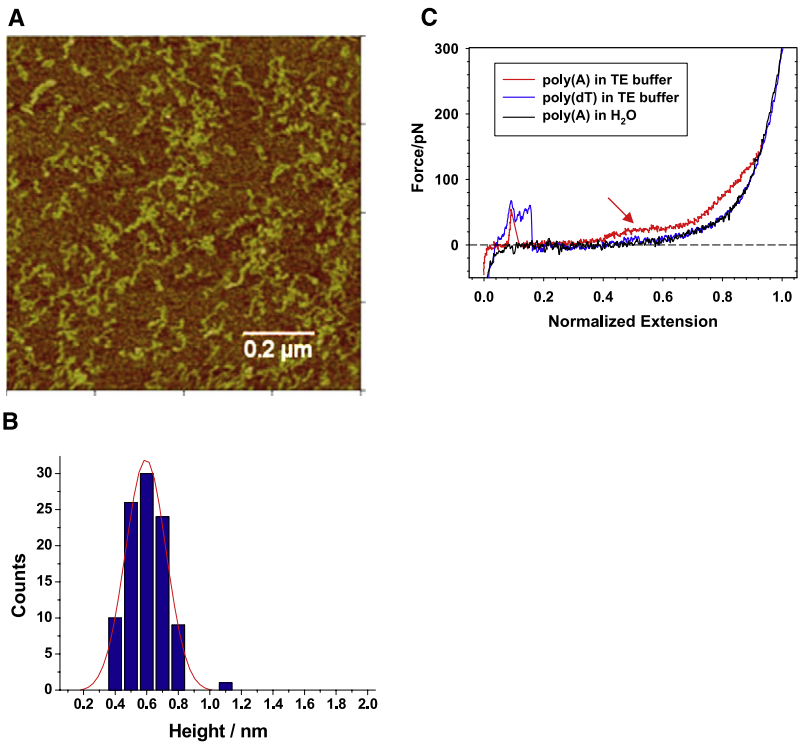

FIGURE 1 (*A*) An AFM image of poly(A) at a pH of 8.0. TE buffer was supplemented with 150 mM NaCl. The image size is 1 μm $\times$ 1 μm. (*B*) The height histogram of 100 poly(A) molecules from the image shown in *A*. (*C*) A comparison of force-extension curves of poly(A) and poly(dT) in TE buffer, and poly(A) in deionized water (pH 5.5). The extension was normalized at a common force of 300 pN .

becomes even more visible when the recording is contrasted with the force-extension profile of polydeoxythymidylate (poly(dT) (Fig. 1 *C*, *blue curve* (*dark gray* in print)). The elasticity of poly(dT) is represented by a simple monotonically increasing force-extension curve (4) that is characteristic of worm-like chain (WLC) polymers. This purely entropic spring behavior of poly(dT) is consistent with the absence of base-stacking interactions among thymines (30).

We also measured the elasticity of poly(A) molecules immersed in pure Mili-Q water (pH ~5.5). One representative force-extension recording is plotted as a black curve in Fig. 1 *C*. It can be seen that this elasticity profile is indistinguishable from the elasticity profile of poly(dT). This observation suggests that poly(A) molecules are in a single-stranded, random-coil conformation in pure water. Thus, the acidic pH alone is not enough to promote the formation of double-stranded structures by poly(A). It seems that, in similarity to native dsDNA (16), a minimum ionic strength of solution is also required to maintain double-stranded structures of poly(A).

AFM imaging of poly(A) under mildly acidic pH conditions

We performed AFM imaging of poly(A) deposited from citrate buffer supplemented with 150 mM NaCl, at a pH of 5.5. A representative AFM image showing the height of poly(A) molecules is displayed in Fig. 2 *A*. It can be easily seen from this figure that poly(A) forms a variety of structures with different heights and lengths in such acidic buffer conditions. This variety is reflected in the histogram of heights (Fig. 2 *B*), which shows two broad populations centered at 0.55 ± 0.013 nm and 1.12 ± 0.022 nm ($n = 100$). A height of 0.55 nm indicates a single-stranded conformation (compare with Fig. 1, *A* and *B*), whereas a height of 1.12 nm is indicative of a dspoly(A) structure. Given the lack of complementary sequences, along with the polydisperse length of poly(A), it should be noted that double-stranded conformations with interspersed single-stranded regions are also expected.

The images shown in Figs. 1 *A* and 2 *A* were obtained from samples deposited from solutions with a low poly(A) concentration of 5–8 ng/μL. However, pulling experiments are typically done on samples deposited from solutions with a higher poly(A) concentration of 50–80 ng/μL. To test whether increased poly(A) concentration at acidic pH conditions changes poly(A) structures, we performed imaging on a sample that was deposited from a solution of poly(A) at a concentration of 40 ng/μL. In this case, the substrate was heavily washed to decrease surface coverage by poly(A) to conditions suitable for AFM imaging. A sample image is shown in Fig. 3 *A*). A histogram of the heights of 76 imaged poly(A) molecules is plotted in Fig. 3 *B*). There are clearly two peaks in the distribution. The average heights for the two peaks are $1.17 \pm .053$ nm and $2.49 \pm .032$ nm. As previously observed, the majority of the molecules are in double-stranded conformations (height of 1.17 nm). In addition, a new population is observed with a height of 2.49 nm, indicating that larger poly(A) complexes with more than two poly(A) strands are formed at higher poly(A) concentrations. The various poly(A) structures formed in mildly acidic pH buffer conditions are expected to produce various types of elasticity profiles.

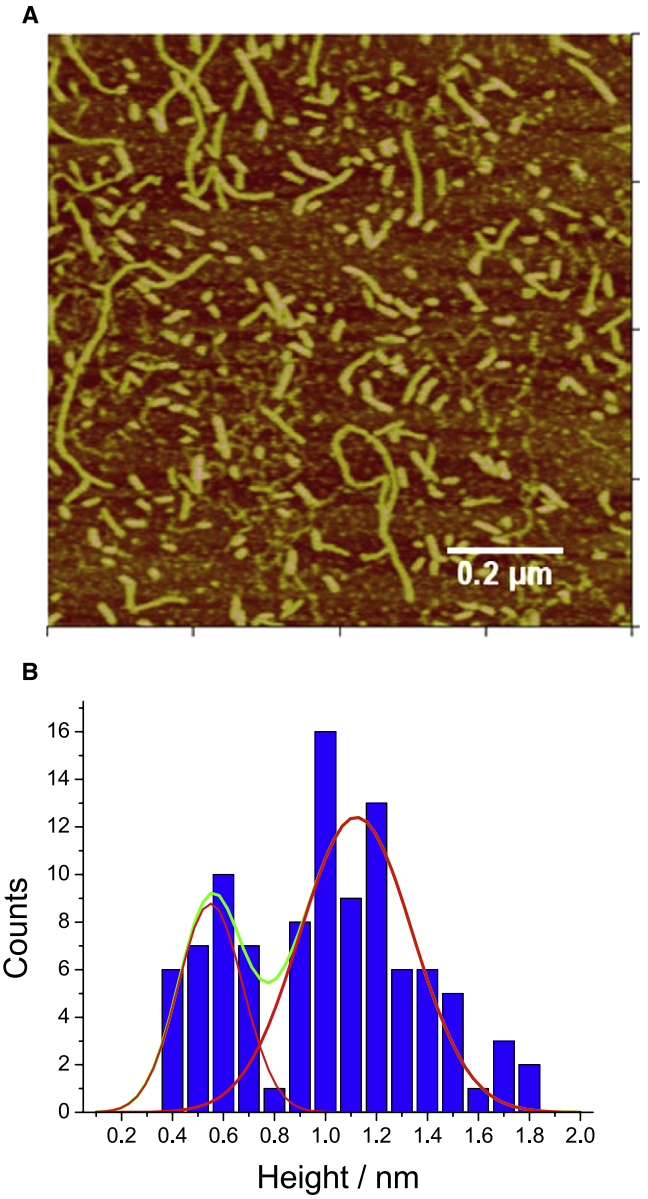

FIGURE 2 (*A*) An AFM image of poly(A) at a pH of 5.5. Citrate buffer was supplemented with 150 mM NaCl. The image size is 1 μm $\times$ 1 μm. (*B*) The height histogram of poly(A) molecules from the image shown in *A*.

Elasticity of poly(A) under mildly acidic pH conditions

The results of force-spectroscopy measurements of poly(A) in citrate buffer (pH 5.5, supplemented with 150 mM

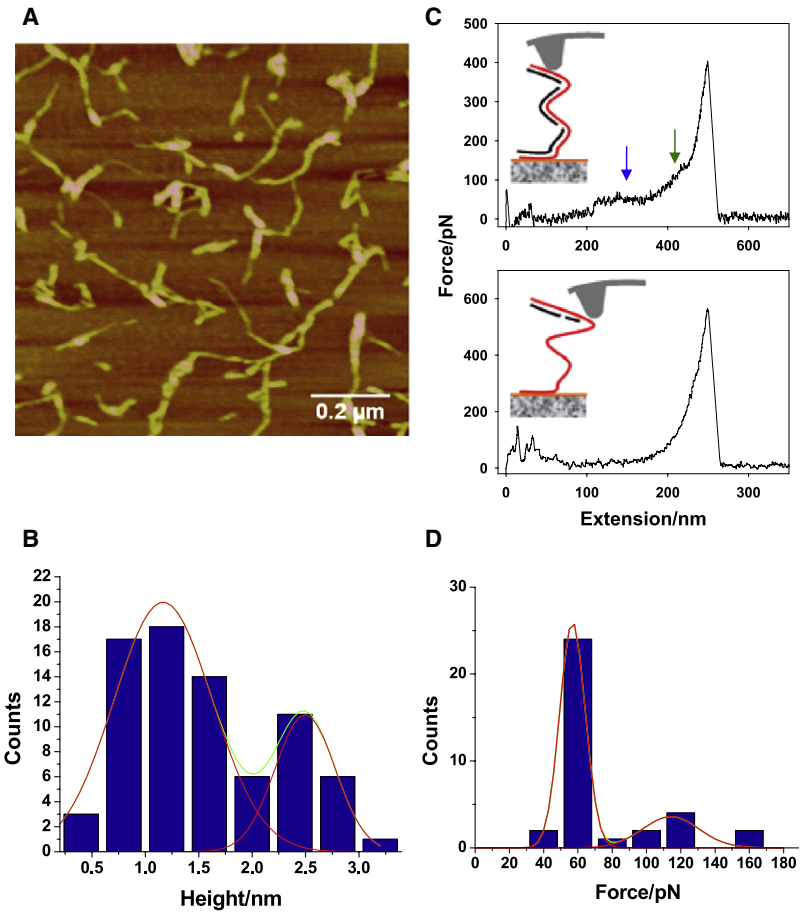

FIGURE 3 (*A*) An AFM image of poly(A) at a pH of 5.5 with a poly(A) solution concentration of ~40 ng/μL. Citrate buffer was supplemented with 150 mM NaCl. The image size is 1 μm × 1 μm. (*B*) The height histogram of poly(A) molecules from the image shown in *A*. (*C*) Representative force-extension profiles of poly(A) measured in citrate buffer. The insets show greatly simplified molecular arrangements of poly(A) corresponding to their respective force curves. (*D*) Histogram of first plateau forces for poly(A) in citrate buffer.

NaCl) are shown in Fig. 3 *C*. The upper elasticity profile, exemplified in Fig. 3 *C*, exhibits two interesting features: a pronounced plateau at 56.8 ± 1.3 pN (*blue arrow* (*dark gray* in print)) (the number of different molecules examined, $n = 35$) and a second plateau at ~130 pN (*green arrow* (*gray* in print)). The first plateau is similar to the so-called B-S transition, whereas the second plateau is similar to the so-called melting transition, both of which are observed in force-extension curves of native dsDNA at ~65 pN (12,17,19,20,28,31–33) and 150 pN (16,28), respectively. The lower-force plateau in the force-extension curves of poly(A) overstretches the molecules by ~75%, as determined by the WLC fits to the data before and after the transition. This extension is similar to the ~70% elongation observed for dsDNA. Similarly, using the WLC fits, we determined that the high-force plateau represents an additional ~20% elongation of the molecule. The similarity between the elasticity of poly(A) measured in citrate buffer to the elasticity of dsDNA strongly suggests that under these conditions poly(A) can indeed be in a double-helical configuration. We note that the histogram of the first plateau force shown in Fig. 3 *D* also includes a minor fraction of forces centered at ~114 pN. This fraction may represent two dspoly(A) molecules being pulled in parallel. Similar effects were previously observed for dsDNA (17).

AFM imaging of poly(A) under acidic pH conditions

To test whether lowering the pH would produce more homogeneous dspoly(A) structures, we performed AFM imaging of poly(A) deposited from citrate buffer supplemented with 150 mM NaCl at a pH of 4.8. One representative image is shown in Fig. 4 *A*. This image indeed reveals molecules that have a fairly homogeneous appearance when compared with the images in Figs. 2 *A* and 3 *A*. Fig. 4 *B* shows the height histogram of 100 poly(A) molecules captured in four different images. The distribution displays a single peak centered at a height of 1.21 ± .028 nm, confirming the presence of one population consisting primarily of molecules in a double-stranded conformation.

Elasticity of poly(A) under acidic pH conditions

To illustrate the effect of lower pH on poly(A) elasticity, we performed force-spectroscopy measurements in citrate buffer at a pH of 4.8. A sample of force curves can be seen in Fig. 4 *C*, and a histogram of plateau forces for 78 force curves is shown in Fig. 4 *D*. The majority of plateau forces averaged 66.7 ± 1.0 pN, which is closer to the plateau force of dsDNA compared to poly(A) at pH 5.5, which had a plateau force of ~57 pN. There is also a small minority of

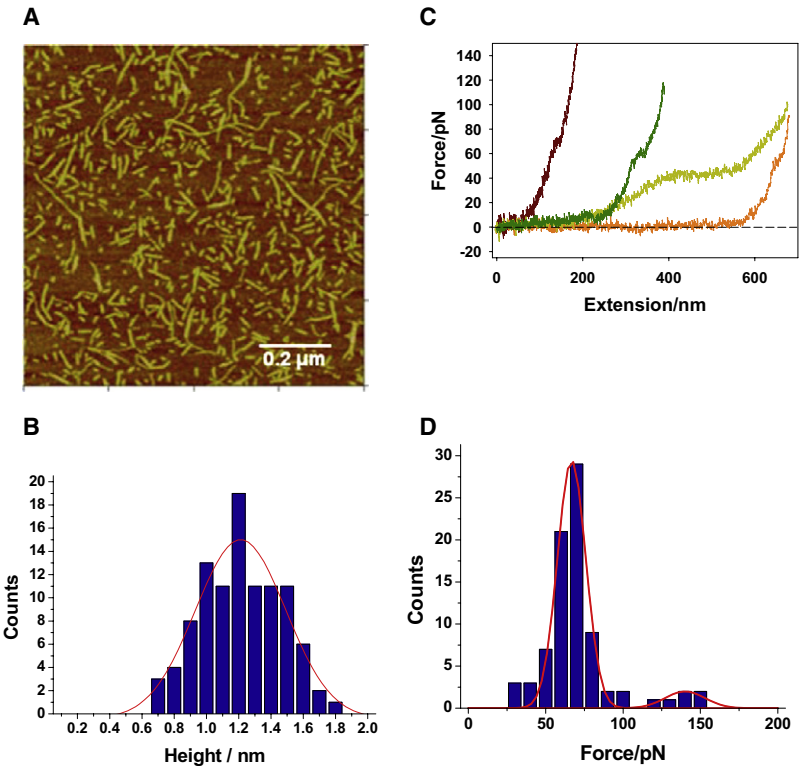

FIGURE 4 (*A*) An AFM image of poly(A) at a pH of 4.8. Citrate buffer was supplemented with 150 mM NaCl. The image size is 1 μm × 1 μm. (*B*) The height histogram of molecules from the image shown in *A*. (*C*) Representative force-extension profiles of poly(A) measured in citrate buffer at pH 4.8. (*D*) Histogram of first plateau forces for poly(A) in citrate buffer at pH 4.8.

molecules with an average plateau force of 140.1 ± 1.4 pN, indicating that occasionally two molecules were being pulled in parallel. A noteworthy feature of the displayed force curves in Fig. 4 *C* is the variation in plateau length. This is contrary to AFM imaging, which shows a fairly homogeneous dspoly(A) population at pH 4.8. One reason for this discrepancy may be that poly(A) structures have different binding preferences for the substrates used for pulling versus those used for imaging. It is possible that single-stranded poly(A) fragments bind more readily than double-stranded structures to gold, and thus overrepresent, in pulling measurements, the fraction of hybrid molecules composed of double strands with single-stranded fragments.

In Fig. 5 we show force spectroscopy measurements in which the relaxing trace was also captured. In such cases a pronounced hysteresis between the stretching and relaxing traces was recorded. Such a hysteresis persisted for several consecutive pulling cycles on the same molecule. The hysteresis shown in Fig. 5 suggests that one strand of the double helix could be peeled off during the stretching process and partially reannealed during the relaxing process (32). It is also noted that the transition between the baseline and the low-force plateau in the stretching part of this force extension curve is less sharp compared with that shown in Fig. 3 *C*. We propose that this gradual transition feature represents yet another structural arrangement in dspoly(A), in which there is a significant single-strand gap(s), as illustrated in the inset in Fig. 5. Therefore, the force-extension curve of a hybrid structure composed of a single-stranded segment(s) connected in series with a double-stranded section(s) is expected to be a linear combination of the respective elasticity profiles for both structures, and should display a less sharp transition. This hypothesis is also supported by the observation that the plateau width in Fig. 5 is reduced to ~55% of the initial length, as compared with the 70%–80% observed in other cases (Fig. 3 *C*). Fig. 6 shows a series of force spectrograms of consecutive stretching and relaxing of the same poly(A) molecule in citric buffer (pH 5.5, supplemented

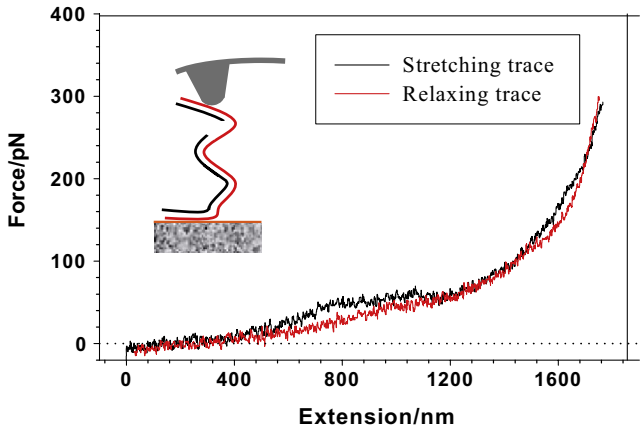

FIGURE 5 A comparison between the stretching (*black*) and relaxing (*red* online; *gray* in print) traces of a dspoly(A) structure. The inset illustrates the possible strand arrangement inferred from the force-extension relationship. The pulling time for one cycle, including both stretching and relaxing of the molecule, is 7.0 s.

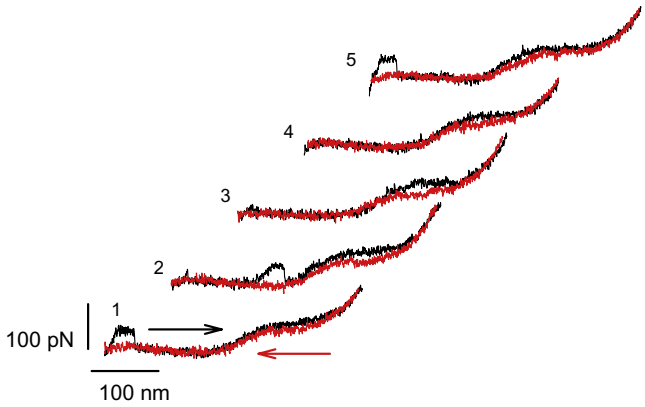

FIGURE 6 Five consecutive stretching and relaxing measurements of the same poly(A) molecule at pH 5.5 in citrate buffer. The black traces represent stretching, and the red traces (*gray* in print) represent relaxation during the cycle.

with 150 mM NaCl). In this experiment, the extension of the poly(A) molecule was limited to keep the magnitude of the pulling force below the value at which poly(A) is expected to undergo the melting transition. Our results show that there is less hysteresis between the traces compared with the hysteresis observed on molecules being stretched beyond their melting transitions, as shown in Fig. 5.

DISCUSSION

Taken together, the results of the AFM imaging and pulling measurements on poly(A) structures presented here are consistent with previous x-ray fiber diffraction data showing dspoly(A) structures (7). It seems that such double helices are mechanically comparable to native DNA duplexes. This is an interesting and somewhat counterintuitive result because poly(A) structures are supposed to be stabilized by four hydrogen bonds, rather than two to three hydrogen bonds per basepair as in native DNA (2). It must be noted, however, that the analogy between the mechanics of dsDNA and dspoly(A) is limited because there are several significant structural differences between the two polymers. The former has two strands oriented in an antiparallel configuration, whereas in the latter both strands run parallel. Also, whereas native DNA exists in the B-form with the C2′ endo sugar pucker, poly(A) is thought to be in the A-form with the C3′ endo sugar pucker, and cannot exist in the B-form because of the presence of 2′-hydroxyl (34). In addition, as documented by AFM imaging (Fig. 2 *A*), poly(A) chains, unlike native dsDNA, even under the same solution conditions form a variety of double-stranded structures. This is because poly(A) strands have different lengths (are polydispersed), and the extent to which two strands overlap in a duplex may, in the absence of sequence specificity, vary from one structure to another. This situation is schematically shown in the insets in Fig. 3 *C*, which illustrate some possible chain arrangements. Different chain arrangements and the resulting structural imperfections, such as single-strand breaks or single-strand gaps in the double-stranded structures, may produce different force-extension curves when these structures are stretched in AFM. This explains why the force curves in Fig. 4 *C* have such a variety of plateau lengths. Indeed, in ~40% of AFM recordings that may be attributed to individual dspoly(A) structures, we observed elasticity profiles somewhat different from the one shown in Fig. 3 *C*, with a significantly reduced width of the first force plateau.

The forced-conformational transition in poly(A) is less cooperative than the B-S overstretching transition in dsDNA

Our results reveal that the low-force plateau in the force spectrograms of dspoly(A) displays a finite slope. For instance, the transition captured in Fig. 5 occurred within 10 pN as measured along the 445-nm-wide overstretching extension corresponding to this force plateau. For comparison, in dsDNA, the B-S transition occurs within 2 pN, which is indicative of a highly cooperative nature of this transition. Thus, it is possible that the transition in dspoly(A) is less cooperative than that in dsDNA. It is also possible that the wider force range of this transition also reflects the contribution to the overall elasticity of the structure originating from single-stranded pieces within dspoly(A), as discussed above.

High-force plateau of poly(A)

As mentioned earlier, at forces >150 pN, native dsDNA undergoes the so-called melting transition in which the two strands are believed to separate. The high-force plateau captured for dspoly(A), as shown in Figs. 3 *C* and 5, could also be produced by a similar mechanism. An alternative explanation may be found by considering the forced conformational transition in the ribofuranose rings from their C3′ endo pucker (5.9 Å spacing between the neighboring phosphates) to a C2′ endo pucker (7 Å spacing between the neighboring phosphates) (4). Such a transition theoretically would produce an 18.5% elongation of the molecule, which agrees well with our WLC-based estimates for this transition (~20%). Therefore, the forced sugar puckering transition seems a plausible explanation for the high-force plateau. The fact that such a transition is not observed in single-stranded poly(A) (Fig. 1) could be explained by assuming that in long single-stranded poly(A), the ribofuranose rings are already in the extended C2′ endo pucker. Surprisingly, reliable data on the ribofuranose pucker in long single-stranded poly(A) structures are unavailable in the literature. Further studies including the determination of ribofuranose pucker in long poly(A) structures, as well as long time-steered molecular-dynamic simulations of the stretching process (35), are warranted to decipher the molecular events captured by the two force plateaus in the force-extension profiles of dspoly(A).

In addition to measurements with pH values of 5.5 and 4.8, we performed some pulling measurements on poly(A) with the pH of the buffer lowered to 4.0. Previous studies showed that poly(A) molecules are in double-stranded configurations in such acidic pH conditions (2), and that they easily form larger complexes or aggregates. Force-extension recordings captured on poly(A) under such conditions showed complex elasticity profiles that lacked easily recognizable and repeatable patterns. This observation is consistent with the above-mentioned tendency of poly(A) to form complicated multistrand structures at such a low buffer pH.

CONCLUSIONS

By means of AFM, we visualized molecular complexes formed by poly(A) under alkaline, mildly acidic, and acidic conditions. We also investigated the mechanical properties of poly(A) at a single-molecule level by atomic force spectroscopy under similar conditions. Both AFM imaging and pulling measurements revealed the complex chain arrangements within poly(A) induced by acidic pH conditions. We determined that among a variety of molecular complexes formed by poly(A) segments, poly(A) forms mechanically stable, double-stranded structures that display elasticity profiles similar to those of native dsDNA. Our results also reveal that single-stranded poly(A) under mildly acidic pH and very low salt conditions behaves like an unstructured, random-coil polymer. This is in contrast to the behavior of this polynucleotide under neutral or alkaline conditions, where it forms quasi-ordered helical structures.

We thank Dr. Alexander Lushnikov and Dr. Yuri Lyubchenko for sharing their APS-mica preparation techniques with us, and Dr. Alexander Gall for providing the APS synthesis protocol.

This work was supported by grants from the National Science Foundation and the National Institutes of Health to P.E.M.

REFERENCES

1. Rottman, F. M. 1978. Biochemistry of Nucleic Acids II. University Park Press, Baltimore, MD.
2. Petrovic, A. G., and P. L. Polavarapu. 2005. Structural transitions in polyriboadenylic acid induced by the changes in pH and temperature: vibrational circular dichroism study in solution and film states. *J. Phys. Chem. B*. 109:23698–23705.
3. Turner, D. H. 2000. Conformational changes. *In* Nucleic Acids: Structure Properties and Functions. V. A. Bloomfield, D. M. Crothers, and I. Tinoco, editors. University Science Books, Sausalito, CA. 259–334.
4. Ke, C., M. Humeniuk, H. S-Gracz, and P. E. Marszalek. 2007. Direct measurements of base stacking interactions in DNA by single-molecule atomic-force spectroscopy. *Phys. Rev. Lett.* 99:018302.
5. Seol, Y., G. M. Skinner, K. Visscher, A. Buhot, and A. Halperin. 2007. Stretching of homopolymeric RNA reveals single-stranded helices and base-stacking. *Phys. Rev. Lett.* 98:158103.
6. Buhot, A., and A. Halperin. 2004. Effects of stacking on the configurations and elasticity of single-stranded nucleic acids. *Phys. Rev. E Stat. Nonlin. Soft Matter Phys.* 70:020902–020904.
7. Rich, A., D. R. Davies, F. H. C. Crick, and J. D. Watson. 1961. The molecular structure of polyadenylic acid. *J. Mol. Biol.* 3:71–86.
8. Holcomb, D. N., and S. N. Timasheff. 1968. Temperature dependence of the hydrogen ion equilibria in poly(riboadenylic acid). *Biopolymers*. 6:513–529.
9. Fresco, J. R., and P. Doty. 1957. Polynucleotides. I. Molecular properties and configurations of polyriboadenylic acid in solution. *J. Am. Chem. Soc.* 79:3928–3929.
10. Zarudnaya, M. I., and D. M. Hovorun. 1999. Hypoterical double-helical poly(A) formation in a cell and its possible biological significance. *IUBMB Life*. 48:581–584.
11. Marko, J. F. 1998. DNA under high tension: overstretching, undertwisting, and relaxation dynamics. *Phys. Rev. E Stat. Phys. Plasmas Fluids Relat. Interdiscip. Topics*. 57:2134–2149.
12. Rouzina, I., and V. A. Bloomfield. 2001. Force-induced melting of the DNA double helix 1. Thermodynamic analysis. *Biophys. J.* 80:882–893.
13. Wang, M. D., H. Yin, R. Landick, J. Gelles, and S. M. Block. 1997. Stretching DNA with optical tweezers. *Biophys. J.* 72:1335–1346.
14. Wenner, J. R., M. C. Williams, I. Rouzina, and V. A. Bloomfield. 2002. Salt dependence of the elasticity and overstretching transition of single DNA molecules. *Biophys. J.* 82:3160–3169.
15. Wuite, G. J. L., S. B. Smith, M. Young, D. Keller, and C. Bustamante. 2000. Single-molecule studies of the effect of template tension on T7 DNA polymerase activity. *Nature*. 404:103–106.
16. Clausen-Schaumann, H., M. Rief, C. Tolksdorf, and H. E. Gaub. 2000. Mechanical stability of single DNA molecules. *Biophys. J.* 78:1997–2007.
17. Cluzel, P., A. Lebrun, C. Heller, R. Lavery, J. L. Viovy, et al. 1996. DNA: an extensible molecule. *Science*. 271:792–794.
18. Leger, J. F., G. Romano, A. Sarkar, J. Robert, L. Bourdieu, et al. 1999. Structural transitions of a twisted and stretched DNA molecule. *Phys. Rev. Lett.* 83:1066–1069.
19. Smith, S. B., Y. Cui, and C. Bustamante. 1996. Overstretching B-DNA: the elastic response of individual double-stranded and single-stranded DNA molecules. *Science*. 271:795–799.
20. Williams, M. C., I. Rouzina, J. R. Wenner, R. J. Gorelick, K. Musier-Forsyth, et al. 2001. Mechanism for nucleic acid chaperone activity of HIV-1 nucleocapsid protein revealed by single molecule stretching. *Proc. Natl. Acad. Sci. USA*. 98:6121–6126.
21. Bensimon, D., A. J. Simon, V. Croquette, and A. Bensimon. 1995. Stretching DNA with a receding meniscus—experiments and models. *Phys. Rev. Lett.* 74:4754–4757.
22. Bustamante, C., Z. Bryant, and S. B. Smith. 2003. Ten years of tension: single-molecule DNA mechanics. *Nature*. 421:423–427.
23. Bustamante, C., S. B. Smith, J. Liphardt, and D. Smith. 2000. Single-molecule studies of DNA mechanics. *Curr. Opin. Struct. Biol.* 10:279–285.
24. Shlyakhtenko, L. S., A. A. Gall, A. Filonov, Z. Cerovac, A. Lushnikov, et al. 2003. Silatrane-based surface chemistry for immobilization of DNA, protein-DNA complexes and other biological materials. *Ultramicroscopy*. 97:279–287.
25. Rabbi, M., and P. E. Marszalek. 2008. Probing Polysaccharide and Protein Mechanics by Atomic Force Microscopy, 1st ed. Cold Spring Harbor Laboratory Press, New York.
26. Ke, C., Y. Jiang, M. Rivera, R. L. Clark, and P. E. Marszalek. 2007. Pulling geometry induced errors in single molecule force spectroscopy measurements. *Biophys. J.* 92:L76–L78.
27. Oberhauser, A. F., P. E. Marszalek, H. P. Erickson, and J. M. Fernandez. 1998. The molecular elasticity of the extracellular matrix protein tenascin. *Nature*. 393:181–185.
28. Rief, M., H. Clausen-Schaumann, and H. E. Gaub. 1999. Sequence-dependent mechanics of single DNA molecules. *Nat. Struct. Biol.* 6:346–349.
29. Florin, E. L., M. Rief, H. Lehmann, M. Ludwig, C. Dornmair, et al. 1995. Sensing specific molecular-interactions with the atomic-force microscope. *Biosens. Bioelectron.* 10:895–901.

30. Saenger, W. 1984. Principles of Nucleic Acid Structure. Springer-Verlag, Berlin.

31. Morfill, J., F. Kühner, K. Blank, R. A. Lugmaier, J. Sedlmair, et al. 2007. B-S transition in short oligonucleotides. *Biophys. J.* 93: 2400–2409.

32. Cocco, S., J. Yan, J. F. Leger, D. Chatenay, and J. F. Marko. 2004. Overstretching and force-driven strand separation of double-helix DNA. *Phys. Rev. E Stat. Nonlin. Soft Matter Phys.* 70:011910.

33. Rouzina, I., and V. A. Bloomfield. 2001. Force-induced melting of the DNA double helix. 2. Effect of solution conditions. *Biophys. J.* 80:894–900.

34. Cantor, C. R., and P. R. Schimmel. 1980. Biophysical Chemistry: Part I: The Conformation of Biological Macromolecules, 1st ed. W.H. Freeman Co., San Francisco, CA.

35. Lu, H., and K. Schulten. 1999. Steered molecular dynamics simulations of force-induced protein domain unfolding. *Proteins.* 35:453–463.